

## Supporting Information

### **Direct Inkjet 3D Printing Microwires with Small Feature Size by Freezing, Sublimation, and Evaporation Induced Colloidal Nanoparticles Self-Assembly Mechanism**

*Hao Guo, Lilan Zhao, Bo Qian\*, Qixin Wu, Rui Wang, Tianxiang Hua, Jing Qin,  
Lingying Li and Xuejun Shi*

**This PDF file includes:**

**Figures S1 to S25**

**Equation S1 to S28**

**Table S1**

**Appendix S1 to S2**

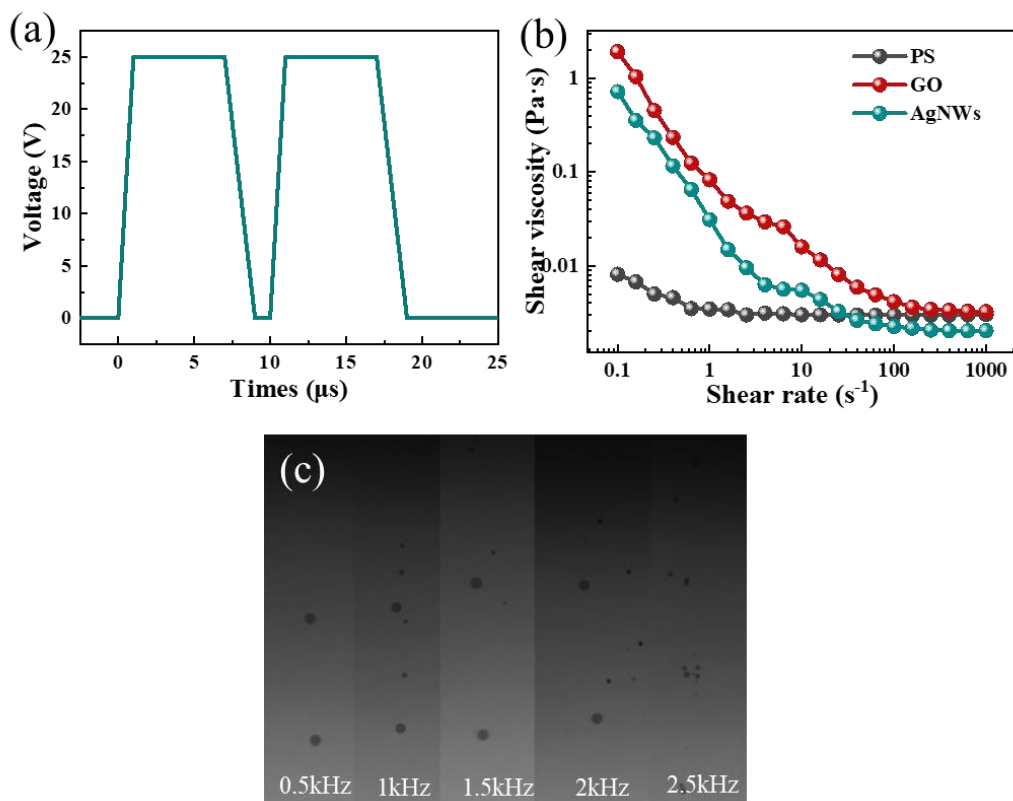


**Figure S1.** (a) Waveform used for ink printing; (b) Ink viscosity varies with shear rate; (c) Jetting photos of PS colloidal particle ink with frequency change.

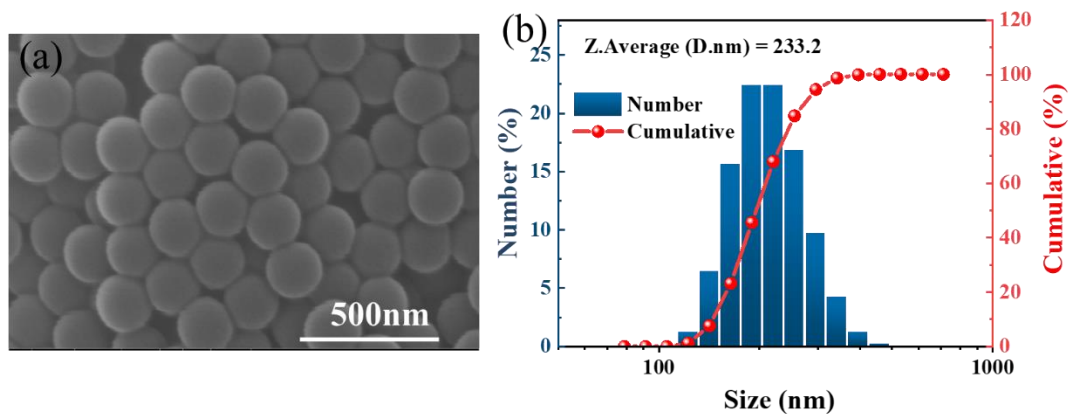


**Figure S2.** (a) SEM of PS colloidal particles. (b) Particle size distribution of PS colloidal particles.

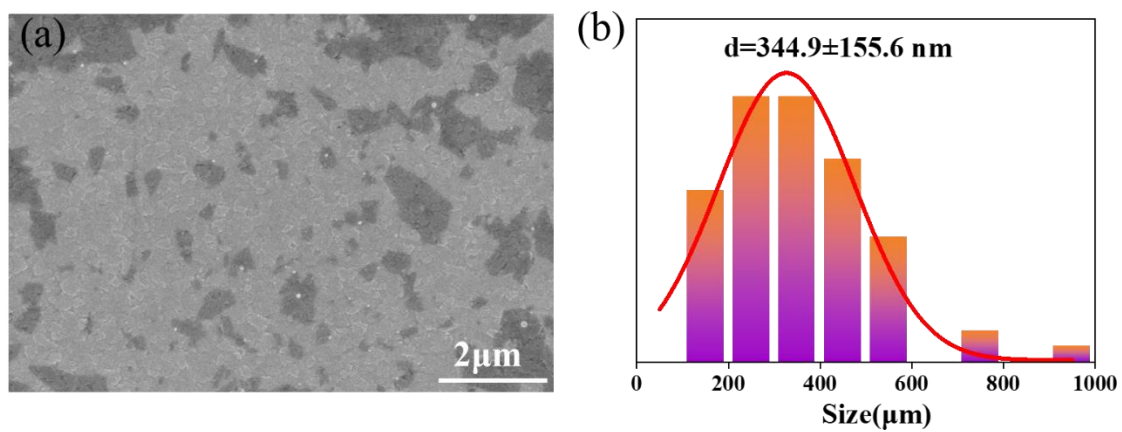


**Figure S3.** (a) SEM of GO sheets. (b) Particle size distribution of GO sheets.

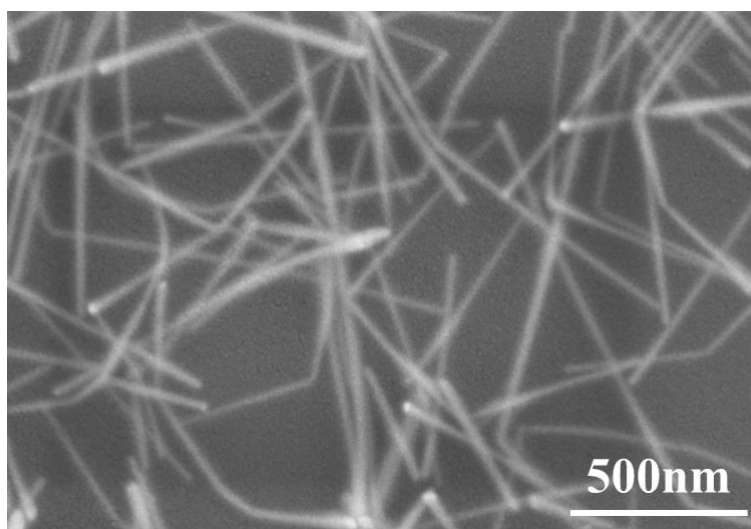


**Figure S4.** SEM of Silver nanowires.

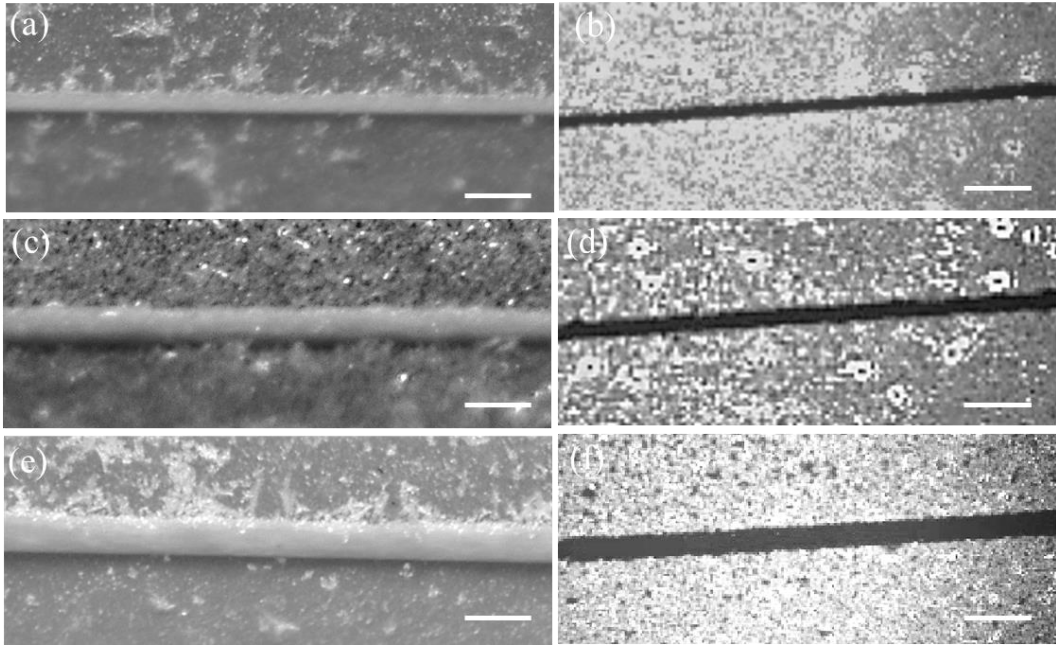


**Figure S5.** (a) Optical microscopy taken at 45° of printed lines with frequency of 200 Hz; (b) Optical microscopy of printed lines with frequency of 200 Hz; (c) Optical microscopy taken at 45° of printed lines with frequency of 500 Hz; (d) Optical microscopy of printed lines with frequency of 500 Hz; (e) Optical microscopy taken at 45° of printed lines with frequency of 500 Hz; (f) Optical microscopy of printed lines with frequency of 500 Hz;

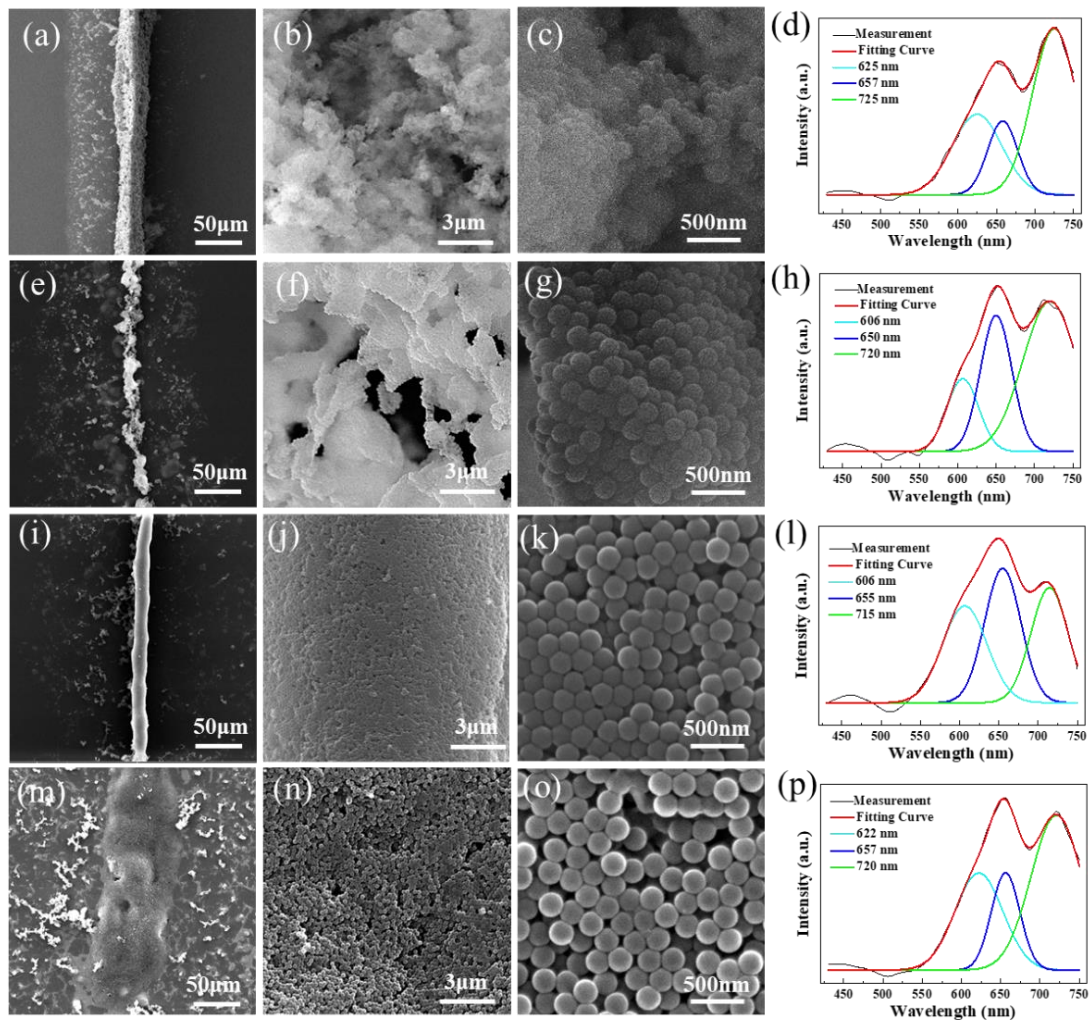


**Figure S6.** SEM images of (a-c) PS+G0, (e-g) PS+G0.6, (i-k) PS+G1.2, and (m-o) PS+G1.5 samples. Micro-reflectance spectra of (d) PS+G0, (h) PS+G0.6, (l) PS+G1.2, and (p) PS+G1.5 samples.

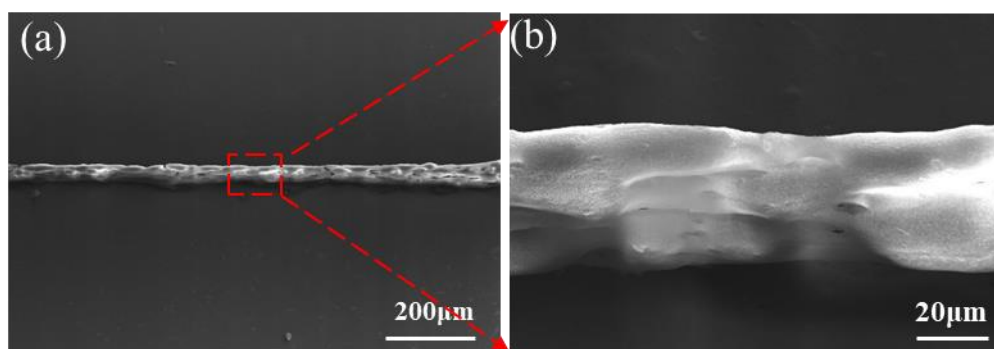


**Figure S7.** (a-b) SEM images of PS-20 wire with the stage tilted at 45°.

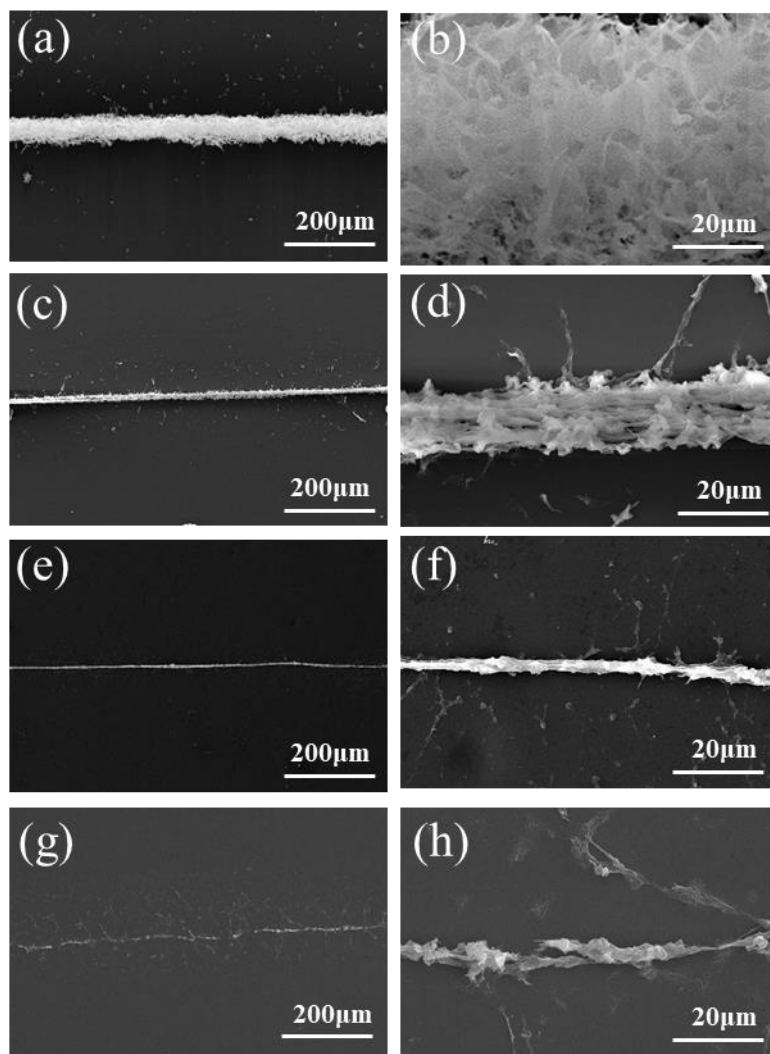


**Figure S8.** SEM images of GO-10 lines with glycerol concentration in inks as (a-b) 0 wt%; (c-d) 1.2 wt%; (e-f) 1.8 wt%; (g-h) 2.4 wt%.

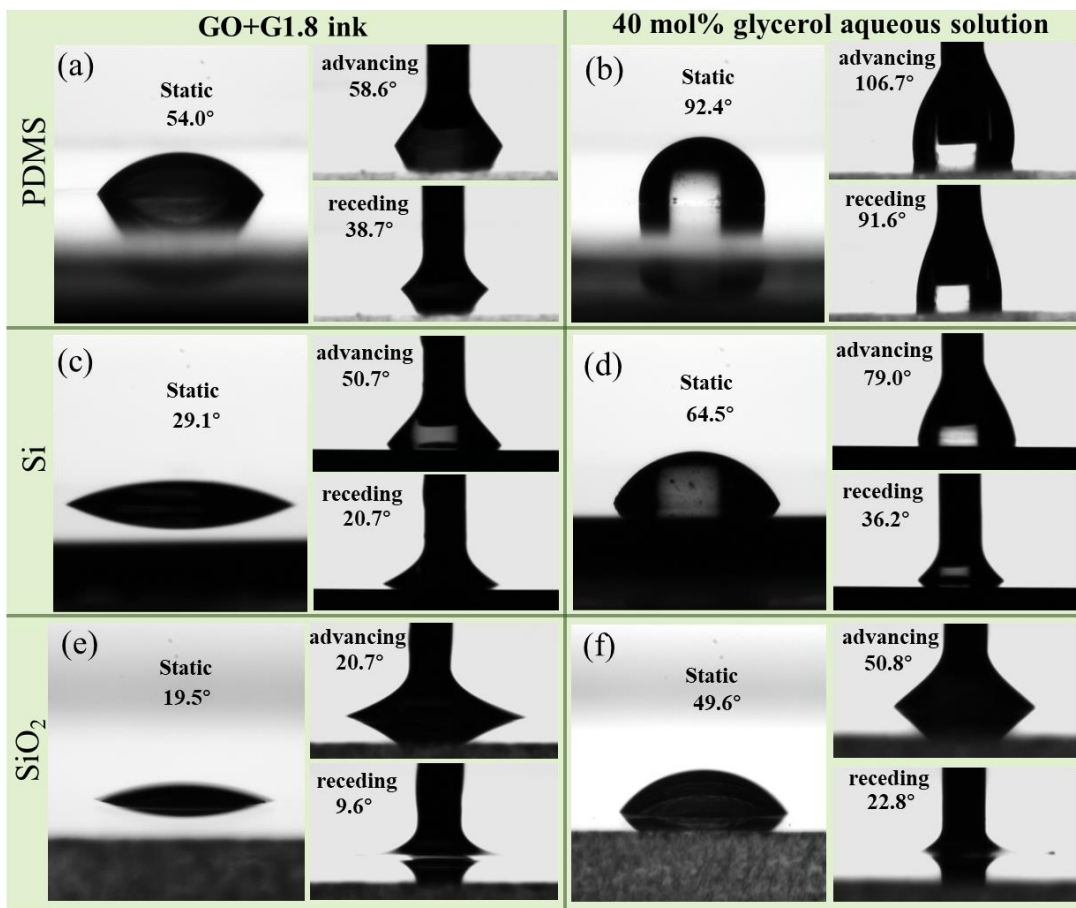


**Figure S9.** Static, advancing and receding contact angles of (a) GO+G1.8 ink on PDMS. (b) Glycerol aqueous solution on PDMS. (c) GO+G1.8 ink on Si. (d) Glycerol aqueous solution on Si. (e) GO+G1.8 ink on SiO<sub>2</sub>. (f) Glycerol aqueous solution on SiO<sub>2</sub>.

Contact angle photography: 1  $\mu$ L liquid droplets were dripped onto the substrate through a micro sampler and filmed by a built CCD system. advancing and receding contact angles were recorded by method of drop growing / shrinking.

Contact angle measurement: tangent method was used to measure the contact angles through a MATLAB program. The code is shown in Appendix 1.

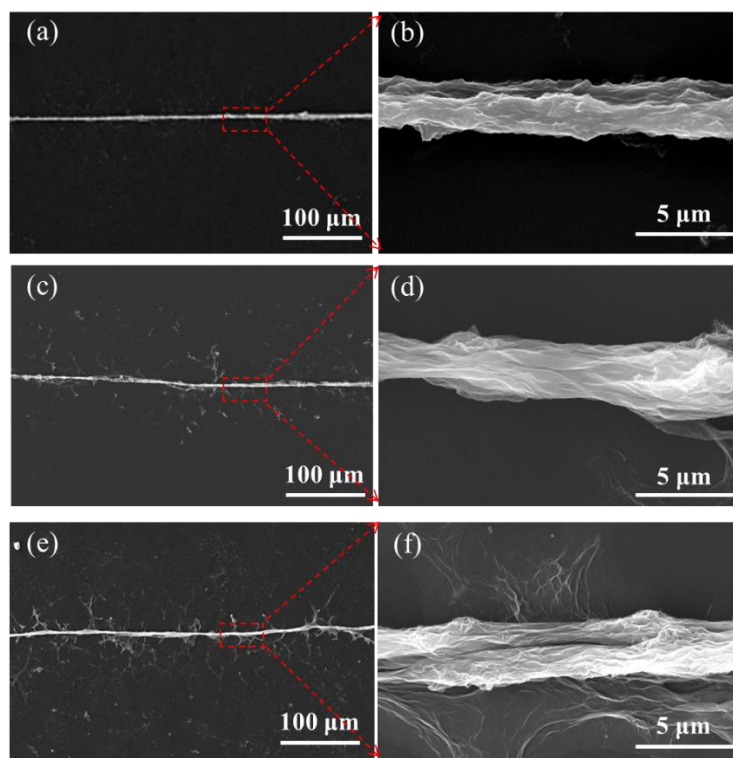


**Figure S10.** Results of GO ink printing on (a-b)PDMS; (c-d)Si; (e-f) SiO<sub>2</sub>.

It can be seen that as the hydrophobicity of the substrate increases, less residue remains on the substrate, so better quality printed lines can be obtained by replacing the more hydrophobic substrate, or hydrophobically treating the substrate.



**Figure S11.** Polarized Microscope photos of 40 mol% glycerol aqueous solution after cryogenic treatment. It can be seen that no crystallization occurs, which illustrates that 40 mol% glycerol aqueous solution exists as a liquid state in the frozen system.

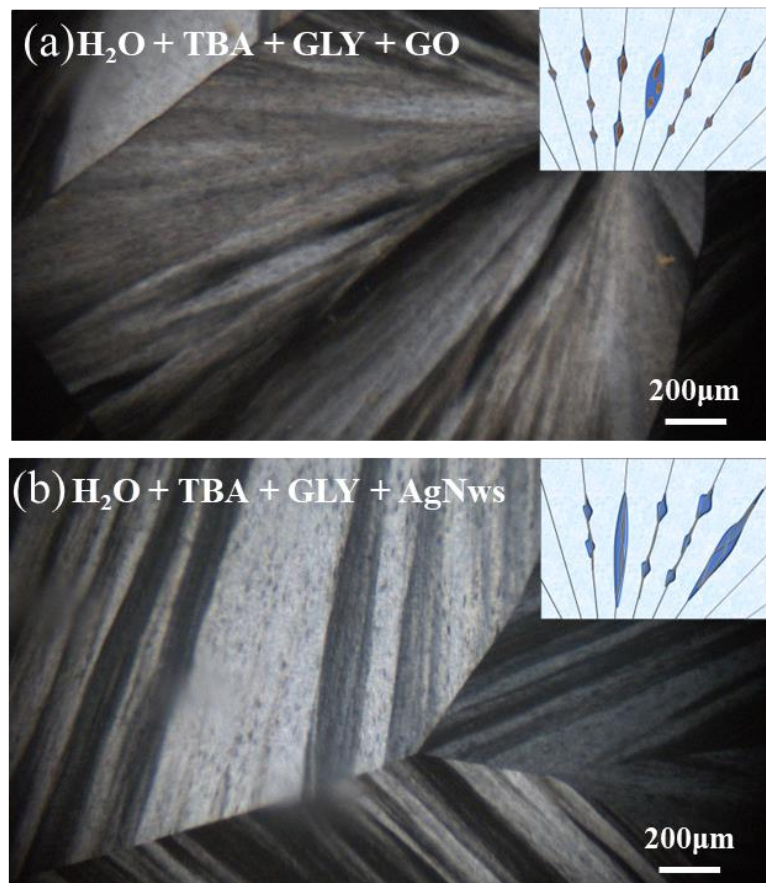


**Figure S12.** Polarized light microscope photograph after cryogenic treatment of (a) GO+G1.8. (b) AgNws+G0.4.

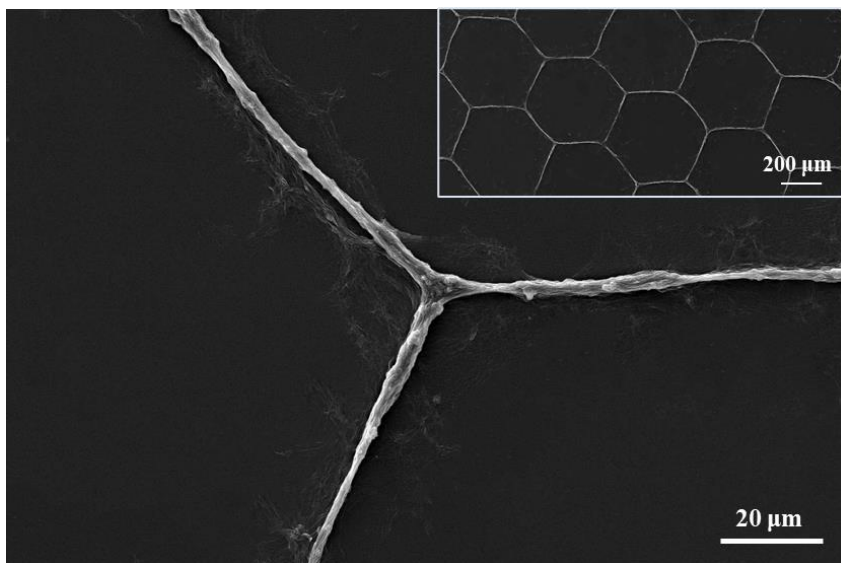


**Figure S13.** Hexagon grid pattern printed in GO-G1.8 ink.

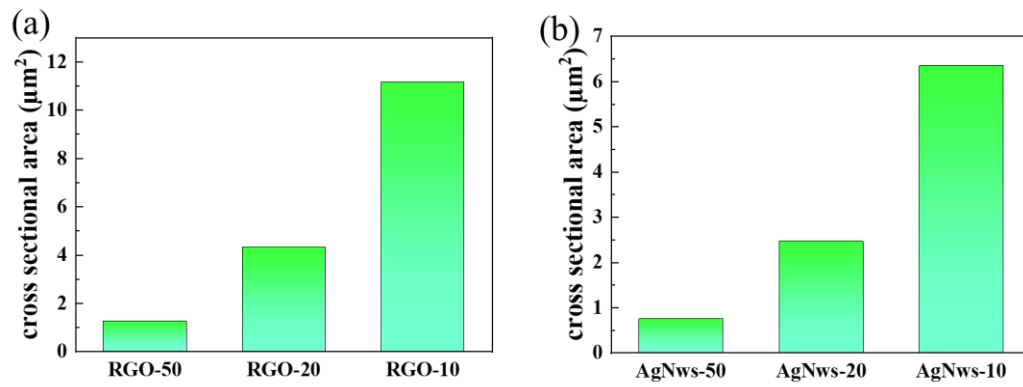


**Figure S14.** (a) Cross-sectional area of the printed RGO wires. (b) Cross-sectional area of the printed AgNws wires.

the resistivity is calculated according to Equation S1 :

$$\rho = RS/L \quad (\text{S1})$$

$\rho$  Is the resistivity.  $L$  is the length of the printed wire,  $S$  is the area, and  $R$  is the resistance value.

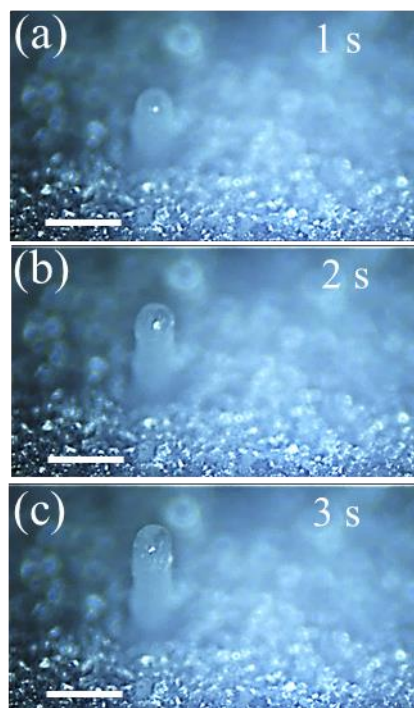


**Figure S15.** (a-c) Cylinder printing process with frequency of 3 Hz, 1s interval per image and scale bar is 200  $\mu\text{m}$ .

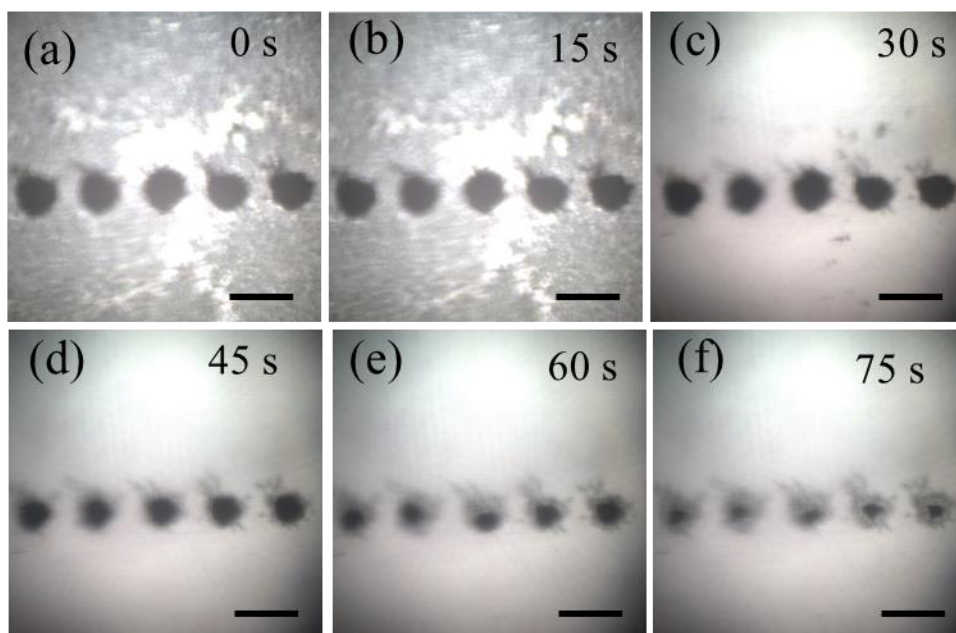


**Figure S16.** (a-f) Sublimation shrinkage process of freezing PS colloidal particle ink cylinder, 15s interval per image and scale bar is 200  $\mu\text{m}$ .

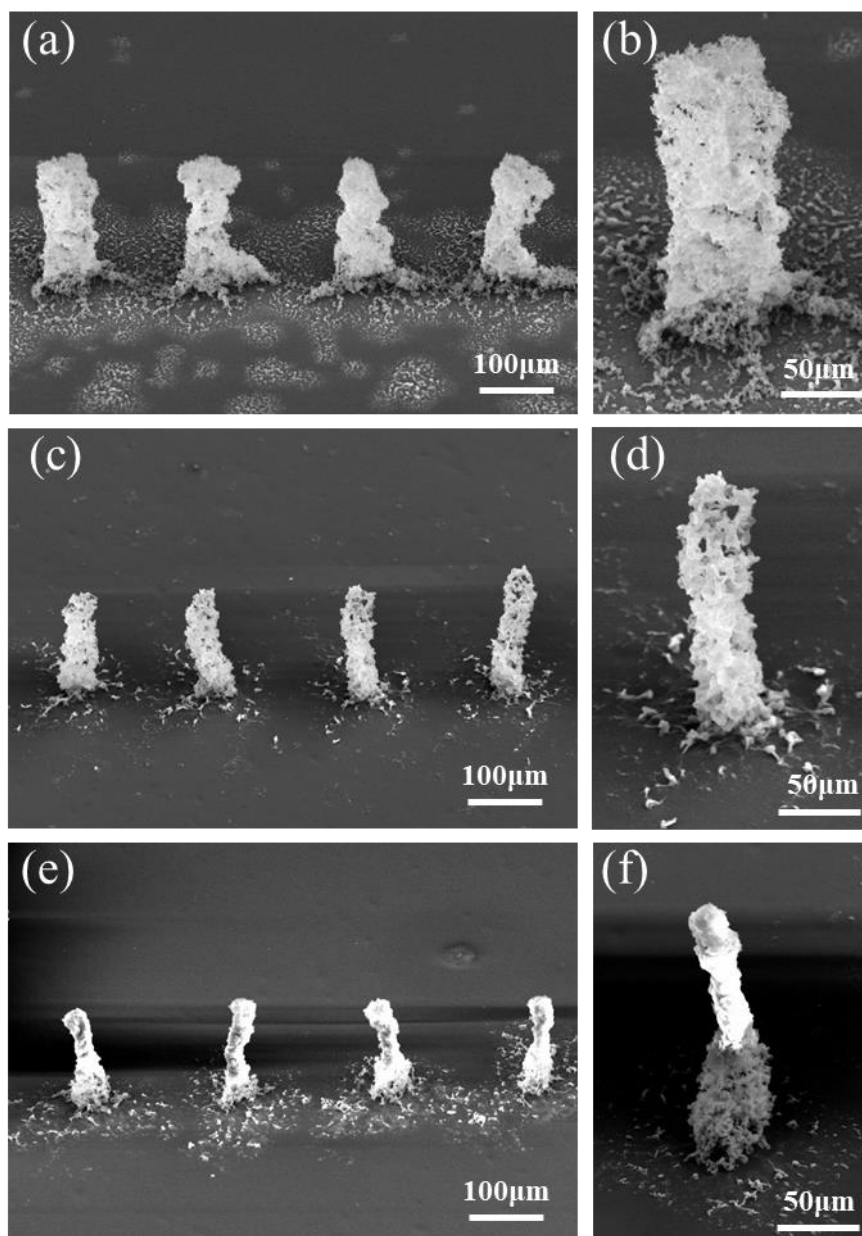


**Figure S17.** SEM images of PS colloidal particles cylinder with glycerol concentration in inks as (a-b) 0 wt%; (c-d) 0.6 wt% ; (e-f) 1.2 wt%.

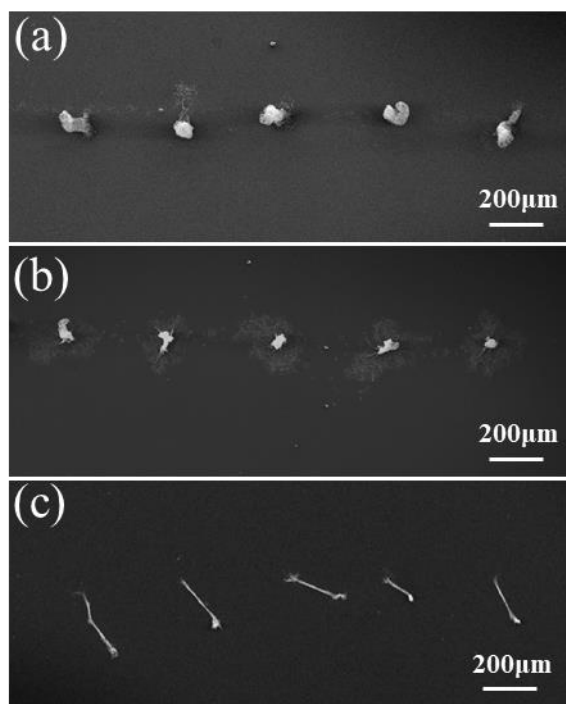


**Figure S18.** SEM images of GO sheets cylinder with glycerol concentration in inks as (a-b) 0wt%; (c-d) 0.6wt%; (e-f) 1.2wt%.

## Simulation of Printing Process

The finite element simulation software COMSOL was used to couple the level set method and non-isothermal flow in multiple physical fields, and then simulate the impact and accumulation process of droplets. In order to simplify the model and improve the calculation efficiency, the kinematics study of printing process was simulated in 2D space, after all the 3D simulation results generation takes long time for CPU speed limitation.

The top of the model (Figure S19) is a droplet generator used to generate droplets at a fixed frequency. The bottom of the model is set to a constant temperature boundary of -40 °C.

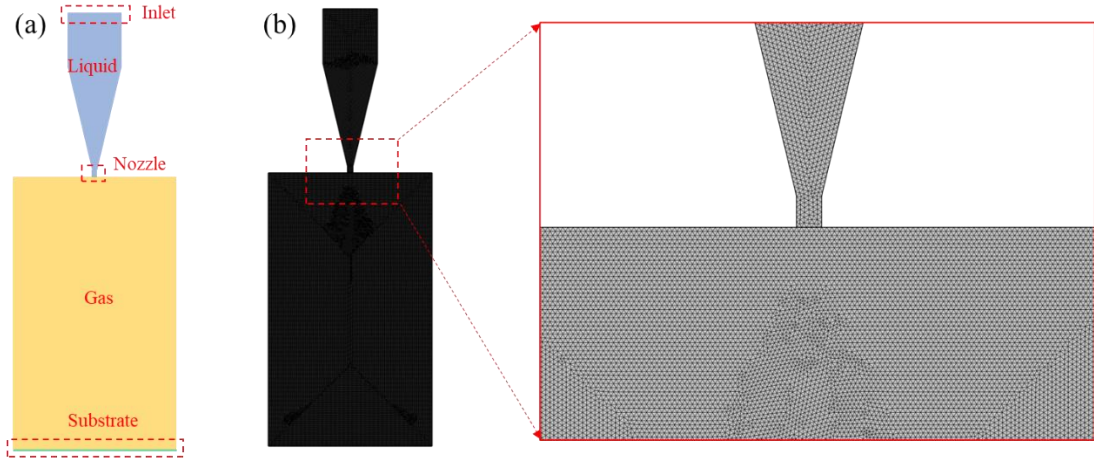


**Figure S19.** (a) Geometric model and (b) Mesh dividing for printing process simulation.

### 1. Physics Governing Equations

#### fluid flow

The incompressible Navier-Stokes equation is used to describe the momentum conservation of fluid. Considering the action of surface tension and gravity, the Navier-Stokes equation can be expressed as:

$$\rho \left( \frac{\partial \mathbf{u}}{\partial t} + \mathbf{u} \cdot \nabla \mathbf{u} \right) - \nabla \cdot \left( \mathbf{u} (\nabla \mathbf{u} + \nabla \mathbf{u}^T) \right) + \nabla p - \rho \mathbf{g} = \mathbf{F} \quad (\text{S2})$$

The continuity equation is expressed as:

$$\nabla \cdot \mathbf{u} = 0 \quad (\text{S3})$$

Where: where  $\mathbf{u}$  is the velocity,  $\rho$  is the density,  $p$  is the pressure,  $\mathbf{g}$  is the

acceleration of gravity.

### Level Set Methods

In order to track the fusion process between droplets, the level set method is used to track the two-phase interface. The basic idea of level set method is to use a high-order function( $\varphi$ ) to describe the motion of gas-liquid interface. The values of  $\varphi$  range from 0 to 1. In this paper, for pure gas phase  $\varphi = 0$ , for pure liquid phase  $\varphi = 1$ ,  $\varphi = 0.5$  represents the two-phase interface. Unit normal vector  $\mathbf{n}$  and curvature  $k$  at the interface are represented by level set function:

$$\mathbf{n} = \frac{\nabla\phi}{|\nabla\phi|} \quad (\text{S4})$$

$$k = \nabla \cdot \frac{\nabla\phi}{|\nabla\phi|} \quad (\text{S5})$$

The motion of the interface can be represented by an improved convection transport equation with the level set function:

$$\frac{\partial\varphi}{\partial t} + \mathbf{u} \cdot \nabla\varphi = 0 \quad (\text{S6})$$

The Heaviside function  $H(\varphi)$  is set to describe the sharp changes of different physical parameters (*density*/ $\rho$ , *viscosity*/ $\mu$ , *thermal conductivity*/ $k$ ) at the phase interface. The liquid phase is assigned as 1 and the gas phase is assigned as 0:

$$H(\varphi) = (1 + \tanh(-\varphi/n))/2 \quad (\text{S7})$$

$$\rho = \rho_g + H(\varphi)(\rho_l - \rho_g) \quad (\text{S8})$$

$$\mu = \mu_g + H(\varphi)(\mu_l - \mu_g) \quad (\text{S9})$$

$$k = k_g + H(\varphi)(k_l - k_g) \quad (\text{S10})$$

Where: Subscript g denotes gas and l denotes liquid.

Surface tension only acts on the gas-liquid interface in the Navier-Stokes equation and is defined by:

$$\mathbf{F}_{\text{ST}} = \sigma\kappa\delta(\varphi)\mathbf{n} \quad (\text{S11})$$

The approximate equation for a given interface width is extended by using the smooth Dirac Delta function:

$$\delta(\varphi) = \frac{n_2}{\sqrt{\pi}} e^{-n_2^2\varphi^2} \quad (\text{S12})$$

## Solidification

Since the substrate temperature (- 40 °C) below ink freezing point(- 5°C, Figure 4g), the droplets will solidify in the process of impacting the substrate, and the solidification is mainly simulated by changing the Navier-Stokes equation. The heat transfer equation of the system is expressed as:

$$\rho c_p \frac{\partial T}{\partial t} + \nabla \cdot (-k \nabla T + \rho c_p T \mathbf{u}) = 0 \quad (\text{S13})$$

The solidification process is very complex, and the enthalpy-porosity method<sup>[1]</sup> is used to simulate this phenomenon: according to the temperature field changes, the calculation domain is divided into three regions: solid region, liquid region and porous region, and porosity.  $\lambda$  Depending on temperature, the whole liquid phase corresponds to a porosity of 1, the whole solid phase corresponds to a porosity of 0, and the solid components solidified by the droplets can be used as a temperature-dependent function  $F_S(T)$  means:

$$F_S(T) = \begin{cases} 0 & T \geq (T_m + \varepsilon) \\ (T_m + \varepsilon - T)/2\varepsilon & (T_m + \varepsilon) > T \geq (T_m - \varepsilon) \\ 1 & T < (T_m - \varepsilon) \end{cases} \quad (\text{S14})$$

Where  $T$  is temperature;  $T_m$  is the solidification temperature of liquid phase, according to the DSC curve of PS ink, the  $T_m$  is taken to be - 5°C;  $\varepsilon$  is half of the freezing temperature range, according to the DSC curve,  $\varepsilon$  is taken to be 5°C.

Corresponding, the porosity is defined as:

$$\lambda = 1 - F_S(T) \quad (\text{S15})$$

In order to incorporate the curing process into the volume force, the solid source term  $S$  is defined as:

$$S = -A \mathbf{u} \quad (\text{S16})$$

Where  $A$  is a function of porosity:

$$A = \frac{C(1-\lambda)^2}{(\lambda^3+q)} \quad (\text{S17})$$

$C$  and  $q$  in the equation are arbitrary constants which can achieve the desired effect. Generally,  $C$  should be large enough and  $q$  small enough. In this paper, the values  $C$  is 5000000 and  $q$  is 0.001.<sup>[2]</sup>

The volume force  $F$  in Equation S2 can ultimately be expressed as:

$$\begin{cases} F_x = \sigma\kappa \frac{\partial\varphi}{\partial x} \delta(\varphi) + S_x H(\varphi) \\ F_y = \sigma\kappa \frac{\partial\varphi}{\partial y} \delta(\varphi) + \rho g_y + S_y H(\varphi) \end{cases} \quad (\text{S18})$$

The total system heat consists of two parts: sensible heat  $h$  and latent heat  $\Delta H$ . The sensible heat is calculated by:

$$h = c_p T \quad (\text{S19})$$

The release of latent heat changes linearly with the decrease of temperature. The enthalpy of phase transition can be written as a function of temperature:

$$\Delta H(T) = \begin{cases} L & T \geq (T_m + \varepsilon) \\ L(1 - F_S) & (T_m + \varepsilon) > T \geq (T_m - \varepsilon) \\ 0 & T < (T_m - \varepsilon) \end{cases} \quad (\text{S20})$$

The latent heat released can be regarded as the sensible heat released only at the transition temperature (from liquid phase to solid phase), so the latent heat capacity can be defined as:

$$c_{pH} = L \delta_{2\varepsilon}(T - T_m) \quad (\text{S21})$$

The improved total heat capacity Equation is:

$$c_{pT} = c_p + c_{pH} \quad (\text{S22})$$

## 2. Physical properties of materials

Table S1 Physical properties of materials

Property	Phase		
	Gas(air)	Liquid(ink)	Substrate(Aluminum)
Density, $\rho/\text{kg}\cdot\text{m}^{-3}$	1.3	966	--
Viscosity, $\mu/\text{mPa}\cdot\text{s}$	0.018	2.35	--
Surface tension, $\sigma/\text{N}\cdot\text{m}^{-1}$	27.4		--
Specific heat, $C_p/\text{J}\cdot\text{kg}^{-1}\cdot\text{K}^{-1}$	1.00	3952	880
Thermal conductivity, $k/\text{W}\cdot\text{m}^{-1}\cdot\text{K}^{-1}$	0.0267	0.602	236
Initial temperature, T/K	293	293	233

## 3. Velocity distribution of droplets during printing

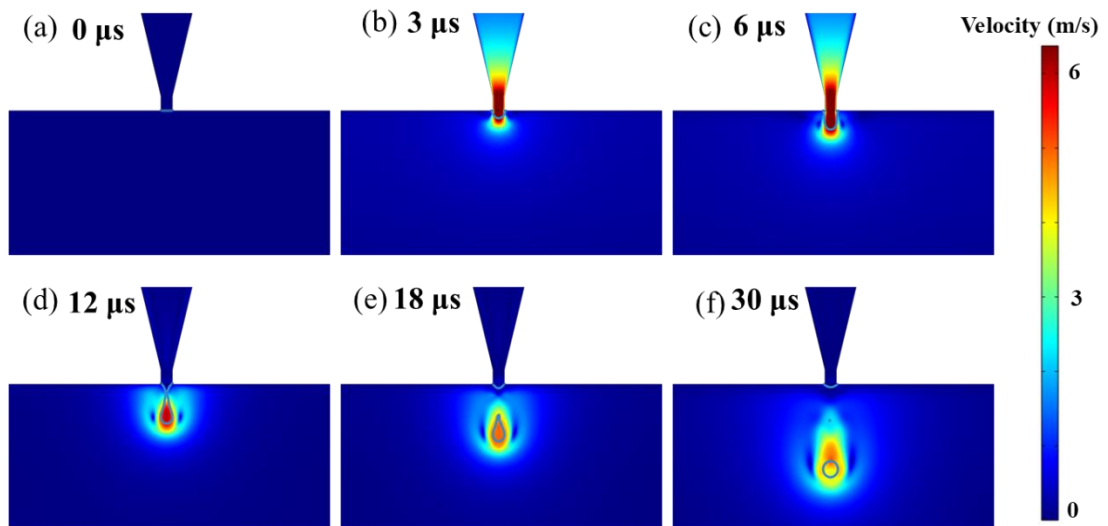


**Figure S20.** Velocity distribution and phase interface migration during ink droplet injection.

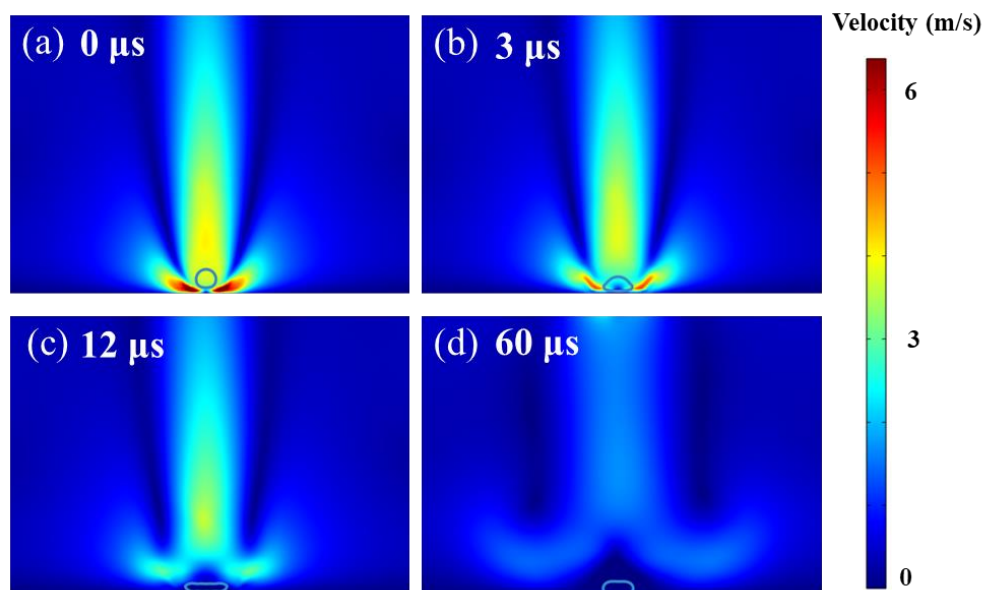


**Figure S21.** Velocity distribution and phase interface migration of ink droplets impacting substrate.

## Sublimation shrinkage process simulation

The sublimation kinetic simulation employs two-dimensional space, and the flow control equations employs Navier-Stokes equations. The dynamic grid method is used for the tracing of the fluid interface.

Stress equilibrium at an air liquid interface:

$$\mathbf{n} \cdot [-p\mathbf{l} + \mathbf{K}] = -p_{ext}\mathbf{n} + \sigma(\nabla_t \cdot \mathbf{n})\mathbf{n} - \nabla_t\sigma \quad (\text{S23})$$

Where  $\mathbf{K} = \mu(\nabla\mathbf{u} + (\nabla\mathbf{u})^T)$  is the viscous stress tensor,  $\sigma(\nabla_t \cdot \mathbf{n})\mathbf{n} - \nabla_t\sigma$  is the force per unit area produced by surface tension.

The relationship between the moving speed of the grid and the mass flow rate  $M_f$  during sublimation is as follows:

$$\mathbf{u}_{mesh} \cdot \mathbf{n} = \left( \mathbf{u} - \frac{M_f}{\rho} \mathbf{n} \right) \cdot \mathbf{n} \quad (\text{S24})$$

The Mass flux ( $M_f$ ) is estimated as  $0.00161 \text{ kg}\cdot\text{m}^{-2}\cdot\text{s}^{-1}$  based on video S2. The calculation procedure is shown in Appendix 2.

The force balance at the contact point is given by Young's equation:

$$\gamma_{s1} + \sigma_{12}\cos\theta_0 = \gamma_{s2} \quad (\text{S25})$$

Where,  $\gamma_{s1}$  is the surface energy per unit area between the fluid 1 and the solid surface.  $\gamma_{s2}$  is the surface energy per unit area between the fluid 2 and the solid surface. The contact angle adopts the receding contact angle of Figure S9b, which is  $91.6^\circ$ ,  $\sigma_{12}$  is the surface tension at the interface between the two fluids, which is  $66.0 \text{ mN}\cdot\text{m}^{-1}$ .

Due to the continuous accumulation of glycerol aqueous solution on the surface during the shrinkage process, the surface of the computational domain is fluid, while the interior is solid. In order to simulate this phenomenon, we linked the change of porosity with the concentration of glycerol:

$$\lambda = 1 - c/cmax \quad (\text{S26})$$

Where:  $c$  is the concentration of glycerol,  $cmax$  is the maximum concentration of glycerol, which is  $7.0\text{mol/L}$  ( $40\text{mol}\%$  glycerol aqueous solution).

Corresponding, the porosity is defined as:

$$\lambda = 1 - F_S(T) \quad (\text{S27})$$

Finally, it is also necessary to define the solid-phase source term  $S$  (Equation S16)

and function  $A$  (Equation S17), and the values of  $C$  and  $q$  are 50000 and 0.001, respectively.

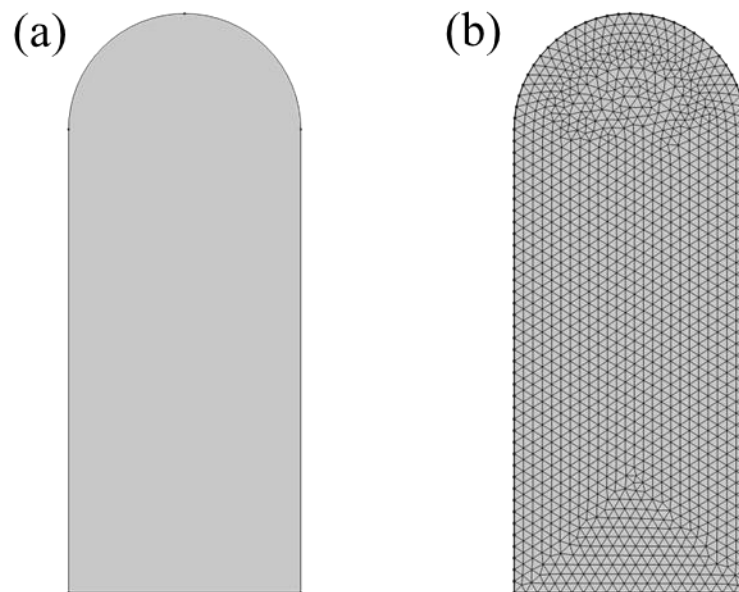


**Figure S22.** (a) Geometric model and (b) Mesh dividing for sublimation simulation.

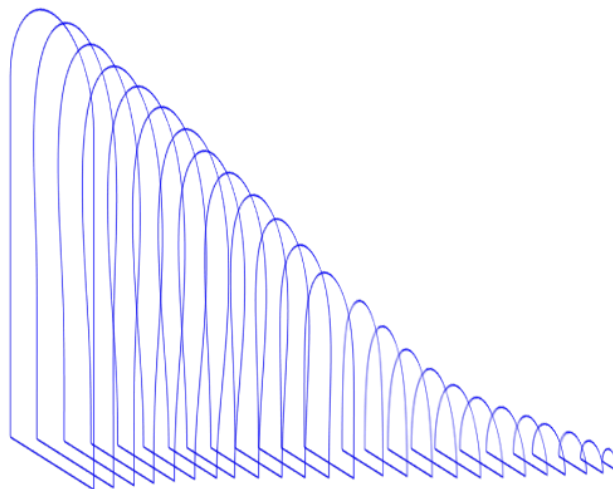


**Figure S23.** Phase interface migration during sublimation

## Appendix S1: Matlab code for measuring contact angle by tangential method

```
clc
cla
clear all
close all
original_picture=imread('C:\Users\Simulation\Desktop\houtuijiao\1.png');%Get
image
imshow(original_picture);
[m,n] = size(original_picture);%Get image size
[x_coordinates, y_coordinates, Pixel_vals] = imread; %Manually define the contact
line between the droplet and the substrate, two-point method
line=polyfit(x_coordinates,y_coordinates,1);%Polynomial fitting, the last 1 represents
the first-order polynomial
xL=1:n;
yL=polyval(line,xL);
hold on;
plot(xL,yL);%Draw baseline by line expression
[x_conic, y_conic, P_conic] = imread; %Quadratic polynomial coordinate picking
conic=polyfit(x_conic, y_conic,2);%Quadratic polynomial fitting
xC=x_conic(1):x_conic(end);
yC=polyval(conic,xC);
hold on;
plot(xC,yC);%Plot by quadratic polynomial expression
xTP=[x_conic(1) x_conic(1)+1];
yTP=polyval(conic,xTP);%Two points of tangent
tangent=polyfit(xTP, yTP,1);%tangent
xT=1:n;
yT=polyval(tangent,xT);
hold on;
```

```

plot(xT,yT);%Draw straight tangent
v1=[xL(1),yL(1)]-[xL(end),yL(end)];
v2=[xT(1),yT(1)]-[xT(end),yT(end)];
angle=acos(sum(v1.*v2)/(norm(v1)*norm(v2)));%Find included angle
contactangle=angle*180/pi;
varname2 = string(contactangle);
text(0.8*n,0.8*m,'contactangle:');
text(0.8*n,0.7*m,varname2);

```

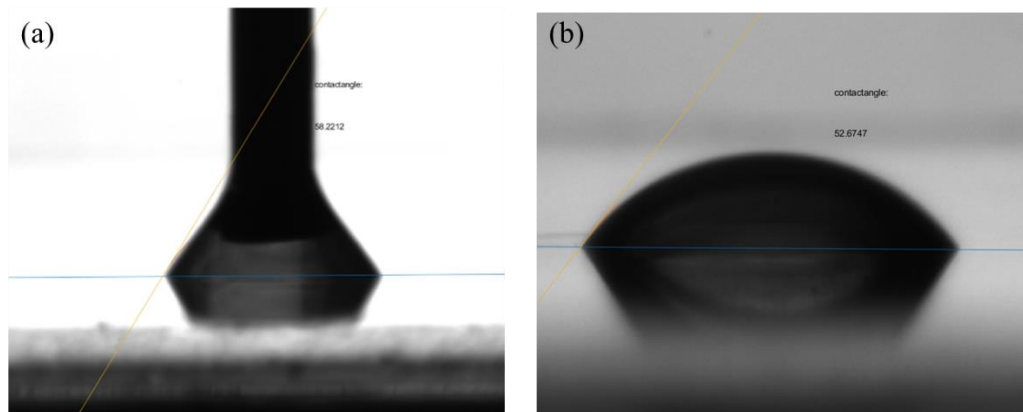


**Figure S24.** (a) Static contact angle measured by tangent method, 49.6°; (b) Receding contact angle measured by tangent method, 22.8°;

## Appendix S2: Mass flux calculation code

The mass flux  $M_f$  during sublimation simulation was estimated from video S2 via Equation S28:

$$M_f = \frac{S_{area}}{\int_0^t t \cdot S_l dt} \quad (S28)$$

Where,  $S_{area}$  is the section area before sublimation,  $t$  is time, and  $S_l$  is the contour curve length of section at each moment. The movement of the outer contour at sublimation is assumed to be in the normal direction. The calculation code as follows:

```
clc
```

```
cla
```

```
clear all
```

```
close all
```

```
xL1=zeros(1,40);
```

```
yL1=0:10:390;
```

```
t_1=0:pi/40:pi;
```

```
t=sort(t_1,'descend');
```

```
xC=100+100*cos(t);
```

```
yC=400+100*sin(t);
```

```
xL2=200*ones(1,40);
```

```
yL2_1=0:10:390;
```

```
yL2=sort(yL2_1,'descend');
```

```
x1=[xL1 xC xL2];
```

```
y1=[yL1 yC yL2];
```

```
plot(x1,y1);%Plot Sample Outline Curve
```

```
[m,n]=size(x1);
```

```
Sarea=trapz(x1,y1);%Calculating graphical area before sublimation
```

```
for j=0:1:n-1
```

```
    for i=0:1:n-2
```

```
        point1{1,1}=[x1.',y1.'];
```

```

M{j+1,1}(i+1,:)=point1{j+1,1}(i+2,1)-
point1{j+1,1}(i+1,1),point1{j+1,1}(i+2,2)-point1{j+1,1}(i+1,2)];
N{j+1,1}(i+1,:)=[-point1{j+1,1}(i+2,2)+point1{j+1,1}(i+1,2),-
point1{j+1,1}(i+1,1)+point1{j+1,1}(i+2,1)];
P{j+1,1}(i+1,:)=N{j+1,1}(i+1,:)/norm(N{j+1,1}(i+1,:));
end %Calculate the normal vector for each contraction
point1{j+2,1}(1,:)=point1{j+1,1}(1,1),point1{j+1,1}(1,2)-
[P{j+1,1}(1,1),P{j+1,1}(1,2)];
for i=1:1:n-2
point1{j+2,1}(i+1,:)=0.9*point1{j+1,1}(i+1,1)+0.1*point1{j+1,1}(i+2,1),0.9*point1
{j+1,1}(i+1,2)+0.1*point1{j+1,1}(i+2,2)]-[P{j+1,1}(i+1,1),P{j+1,1}(i+1,2)];
end %Calculate points after each contraction
point1{j+2,1}(n,:)=point1{j+1,1}(n,1),point1{j+1,1}(n,2)]-[P{j+1,1}(n-
1,1),P{j+1,1}(n-1,2)];
Xpoint(j+1,:)=point1{j+2,1}(:,1);
Ypoint(j+1,:)=point1{j+2,1}(:,2);
for i=0:1:n-2
S0(j+1,i+1) = ((Ypoint(j+1,i+2)-Ypoint(j+1,i+1)).^2+(Xpoint(j+1,i+2)-
Xpoint(j+1,i+1)).^2).^0.5;
end %Calculate the length of the curve after each contraction
S(j+1,:)=sum(S0(j+1,:));
hold on
plot(Xpoint(j+1,:),Ypoint(j+1,:));
Sarea0=trapz(Xpoint(j+1,:),Ypoint(j+1,:));
if Sarea >20*Sarea0
break
end
end
Ssum=sum(S);
t=75/(n-1);

```

```
M=(Sarea-Sarea0)/(Ssum*t*1000);%calculate Mass flux
```

```
hold on;
```

```
text(150,455,'Original area:');
```

```
varname = string(Sarea);
```

```
text(150,425,varname);
```

```
text(160,390,'Mass flux:');
```

```
varname2 = string(M);
```

```
text(160,365,varname2);
```

**result:**

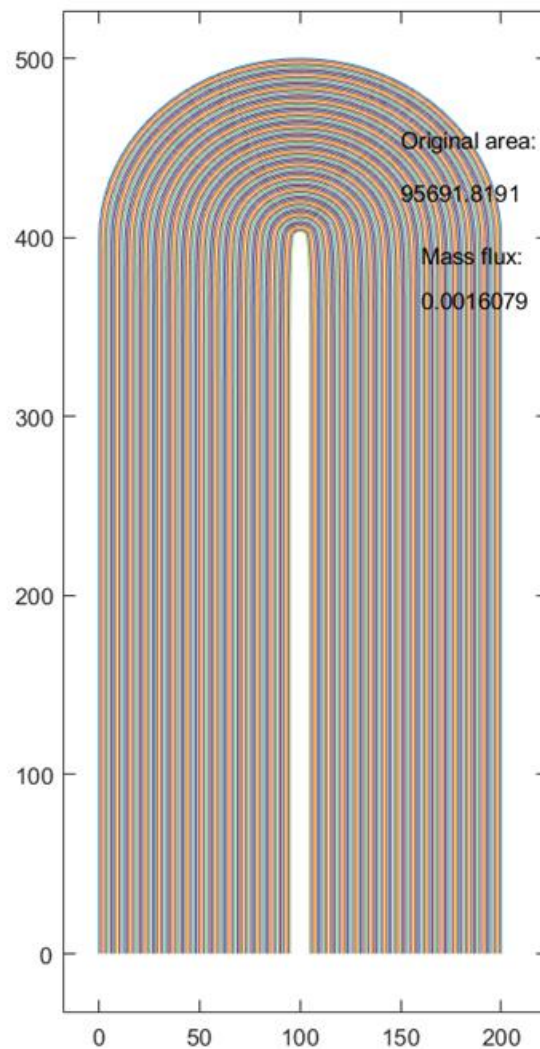


**Figure S25.** Mass flux calculation results

## References

- [1] Q. Ye, S. Chen, *Journal of Manufacturing Science and Engineering* **2017**, 139.
- [2] J. Blake, D. Thompson, D. Raps, T. Strobl, *Aiaa J.* **2015**, 53, 1725.